ELSEVIER

Catalysis Today 53 (1999) 703–713

CATALYSIS TODAY

www.elsevier.com/locate/cattod

Catalysts for sanitary air cleaning from ozone

Tatyana L. Rakitskaya *, A.Yu. Bandurko, A.A. Ennan, V.Ya. Paina

Odessa State University, Physico-chemical Institute of Environment and Human Being Protection, 2, Dvoryanskaya St., Odessa-26, 270026, Ukraine

Abstract

The results of the kinetic study of ozone decomposition over carbon fibrous materials and metal complex compounds ($CuCl_2$) supported on them at ozone concentrations in the 3.1×10^{-8}–3.1×10^{-5} mol/l range are presented. Ozone decomposition occurs mainly in a catalytic way with the steady-state regime attainment depending on CFM physico-chemical as well as structural characteristics and macrokinetic factors of the process. Copper (II) catalyzes decomposition of ozone microconcentrations only. The data obtained can be a base for the development of sanitary air cleaning units and respirators (protective gas-masks).

Keywords: Low-temperature catalysis; Carbon fibrous materials; Copper (II) chloride; Ozone decomposition kinetics

1. Introduction

High toxicity of ozone creates a real menace for the environment and human beings. Various carriers-supported metal, metal oxide and metal oxide-metal catalysts are applied widely in the cleaning of gases from ozone [1,2]. They are similar to those used in the low-temperature air cleaning from carbon monoxide [3]. As a rule, the drawbacks of these catalysts include a complicated composition as well as a high content of noble metal (Pt, Pd) applied to promote the activity of the catalysts and to lower their poisoning by water vapor. Supported metal-complex catalysts are not properly studied in ozone decomposition [4–7].

In our opinion, carbon materials (active carbons (ACs), and carbon fibrous materials (CFMs)) and catalysts on their base are perspective, but also scarcely studied with respect to the low-temperature ozone decomposition reaction. The data of interest relate to ozone interaction with carbon materials as well as the application of the latter as supports of ozone decomposition catalysts. The most complete information about AC-supported oxide catalysts for air cleaning from ozone has been reported in a review [8].

Earlier works [9–11] on ozone interaction with CFMs addressed mainly the kinetic investigations of the accumulation of surface ion-exchange groups of various characters. Nevertheless, the authors have deduced that not only surface oxidation but catalytic ozone decomposition takes place [11]. However, till now, the data concerning kinetics and mechanism of ozone decomposition by CFMs are extremely restricted, and what is more, there are no quantitative criteria to evaluate catalytic activity of CFMs and CFM-supported metal complexes in the reaction. The first attempts to clear up the influence of physical and chemical as well as structural-adsorption properties of CFMs prepared from different materials were: a study of ozone decomposition kinetics within ozone concentration range of 2.1×10^{-7} to 6.3×10^{-7} mol/l [12,13] and a determination of the time of protective

* Corresponding author. Tel.: +380-0482-44-32-93; fax: +380-0482-23-11-16
E-mail address: tanya@farlep.net (T.L. Rakitskaya)

0920-5861/99/$ – see front matter
PII: S0920-5861(99)00157-1

action τ_{MPC} (the time necessary for reaching the maximum permissible concentration of ozone) of these CFMs when $C_{O_3} = 3.1 \times 10^{-8}$ mol/l [14]. The data obtained were used for optimizing CFM application conditions in ozone protecting gas-masks (respirators) [15,16]. However, on the basis of the above-mentioned data, one could not come to more general conclusions permitting to make a purposeful choice of CFM for ozone decomposition. The explanation may lie in that those CFMs differ in a wide spectrum of their physico-chemical and structural-adsorption parameters (a character and a content of surface functional groups, a porous structure, a material width, etc.). In the present study, to diminish a number of variables influencing CFM performance in the reaction, we used CFMs of the same origin material whose properties were set initially.

The aim of the work was to study the dependence of CFM specific activity and the activity of CFM-supported Cu(II) chloro complexes on CFM structural characteristics towards the low-temperature reaction.

2. Experimental

The samples of sorption-active fabric (SAF) type CFMs (Table 1) obtained from the same origin cellulose material were prepared in accordance with a procedure reported [17]: by its impregnation with borax solution (borax served as a structure-forming additive); carbonization at $(800 \pm 30)^\circ$C and activation of different duration in water vapor–CO_2 medium at $(850 \pm 30)^\circ$C. This technique permitted to control a porous structure and other characteristics of CFMs.

The static activity, a_{st}, of these materials was determined through benzene vapor sorption from benzene-air mixture under dynamic conditions at 20°C, $p/p_s = 0.17$ and the volumetric flow rate, $\omega = 5 \times 10^{-5}$ m^3/s. The specific surface of micro- and mesopores, S_{mi} and S_{me}, respectively, and other parameters of the porous structure were determined on the basis of the benzene sorption isotherms applying the equation of the theory of volumetric filling of micropores and calculation methods generally used [18,19]. Since V_{mi} and V_{me} changed simultaneously in the course of CFM activation, we considered V_{mi}/V_{me} as the structural parameter.

Chemical analysis of oxygen-containing groups of CFM surface was made by the back-titration method. The content of acidic groups, A_a, was determined through KOH adsorption and subsequent titration with chlorhydric acid, whereas the content of basic groups, A_b, was evaluated on the basis of HCl adsorption from its aqueous solution following its titration with potassium hydroxide [20].

The developed surface of micro- and mesopores was characteristic for SAF 1-6 carbon fibrous materials; the value of V_{mi}/V_{me} decreased from SAF-1 to SAF-6; their activation led to the predominance of basic groups; the layer thickness was practically invariable ($H = 4 \times 10^{-4}$ m) for the samples [17].

Measurement of pH from water extracts of CFM samples was carried out as follows: 0.5 g of CFM after its size reduction and 20 ml of water were placed into a conical flask with a ground-glass stopper. Then, the flask was shaken for a duration of 1 h; afterwards, the contents were filtered and pH of the filtrate was measured by an ion meter (EV-74 Model).

$CuCl_2$–CFM catalyst samples were prepared on the bases of SAF-1 and SAF-4. Parameters of the porous structure, a character and a content of functional groups differed for them significantly (see Table 1). CFMs were impregnated with aqueous solutions of desirable copper (II) chloride concentrations. The volume of the solution was 1.5 times the total volume of support's pores. This ratio was necessary for the uniform distribution of the catalytic component. The subsequent drying of samples was carried out in air at $T = 100^\circ$C until constant weight. The porous structure of CFM after $CuCl_2$ supporting was controlled by its volume of micropores (V_{mi}). The specific Cu(II) monolayer capacity ($a_{m(Cu)}$) on SAF-1 and SAF-4 surface (2.1×10^{-4} and 2.0×10^{-4} mol/g, respectively) was calculated on the basis of sorption isotherms in Langmuir plot in accordance with the known method [7]. Parameter $a_{m(Cu)}$ was used for calculation of the degree of saturation (β) of the CFM surface with copper(II) chloride: $\beta = C_{Cu(II)}/a_{m(Cu)}$.

Kinetics of ozone decomposition was studied in a temperature-controlled flow system. Gas–air mixtures (GAMs) with desirable ozone concentration were produced by the ozonizer operating with glow discharge in the air purified previously of dust, moisture and nitrogen oxides. Ozone–air mixture, obtained as a result,

Table 1
Structural adsorption and physico-chemical properties of CFMs

CFM	a_{st} (mg/g)	V_{mi} (cm^3/g)	V_{me} (cm^3/g)	V_{mi}/V_{me}	S_{mi} (m^2/g)	S_{me} (m^2/g)	A_a (mmol/g	A_b (mmol/g)	pH
SAF-1	160	0.240	0.035	6.8	780.0	21.2	0.46 ± 0.03	0.21 ± 0.02	6.5
SAF-2	250	0.300	0.070	4.2	930.0	46.1	0.15 ± 0.01	0.40 ± 0.03	7.9
SAF-3	360	0.330	0.100	3.3	1200.0	58.4	absent	0.44 ± 0.03	9.5
SAF-4	333	0.370	0.124	3.0	1300.0	77.5	absent	0.40 ± 0.03	9.0
SAF-5	330	0.350	0.120	2.9	1300.0	77.0	absent	0.52 ± 0.04	9.5
SAF-6	370	0.420	0.210	2.0	1475.0	131.3	absent	0.48 ± 0.03	9.0

was cleaned from NO_x, too. The initial ($C^i_{O_3}$) and final ($C^f_{O_3}$) ozone concentrations up to 30.0 mg/m^3 were measured by a chemiluminescent gas analyzer (3.02P1 Model) with the minimum detectable ozone concentration of 2 $\mu g/m^3$. An optical gas analyzer (Cyclone-Reverse Model) was used for C_{O_3} range of 50 to 1500 mg/m^3. A relative measurement error was within ±15%.

The CFM samples under study were previously dried at 110°C until constant weight. Then, they were placed in brass adapters permitting to regulate GAM linear velocity widely by varying the diameter of an orifice in the adapter and maintaining the volumetric flow rate constant. The reference runs have shown that there is no ozone decomposition on brass walls of the adapter under the experimental conditions. All experimental series were performed at the constant GAM relative humidity $\varphi = 60\%$ except for the experiments where GAM humidity influence was studied.The reaction rate was calculated using the relationship

$$W = \frac{\omega(C^i_{O_3} - C^f_{O_3})}{m}, \quad [\text{mol/g s}] \tag{1}$$

where ω is the volumetric flow rate of GAM, in m^3/s; $C^i_{O_3}$and $C^f_{O_3}$ the initial and the final ozone concentrations, respectively, in mol/m^3; and m the weight of CFM sample, in g, calculated on the basis of CFM surface density and the area of the orifice in the adapter.

CO and CO_2 concentration in GAM in the outlet of the reactor was determined by a gas chromatographic instrument (Gasokhrom 3101 Model) with threshold sensitivity of 1×10^{-3} and 1×10^{-1} vol%, respectively. The basic error of the instrument was within 1.5%.

In the flow reactor with the determined volumetric flow rate of GAM $\omega = 1.7 \times 10^{-5}\ m^3/s$, a laminar flow of reagent (ozone) stream through a single-layer catalyst can be attained. The effective residence time (τ') of GAM was determined as

$$\tau' = \frac{V}{\omega} = \frac{H}{U}, \quad [\text{s}] \tag{2}$$

where V is the total volume of the catalyst layer, ω the volumetric flow rate of GAM, H the height of the catalyst layer, and U the linear velocity of GAM.

The linear velocity of GAM was calculated in consideration of the diameter of the orifice in the adapter:

$$U = \frac{\omega}{S_a}, \tag{3}$$

where S_a is the geometric area of CFM cross section fitting the orifice in the adapter.

3. Results and Discussion

3.1. Influence of diffusion factors and operation conditions of the reactor

Initially, the main criteria of the operating regime of the reactor and the region in which the process occurs were determined. Taking into account a design of the reactor as an adapter with a fastened sample of the catalyst as a woven fabric, it was advisable to consider only the plug-flow regime criteria developed for grain catalysts [21,22], namely, the absence of the axial diffusion and wall effects. The axial diffusion can be neglected when $H/d_{gr} \gg 1$ (d_{gr} is the average grain diameter) [21]. As a characteristic dimension, we have selected the diameter of CFM fiber ($d_f = 6 \times 10^{-6}$ m). Kinetics of a process is not influenced by wall effects if $D_{react}/d_{gr} \geq 30$ (D_r is the inner diameter of the reactor) [21,22]. The data presented in Table 2 show that the requirements mentioned above were held, i.e. the

Table 2
Criteria of axial diffusion and absence of wall effects in the single-layer catalyst sample with an avarage diameter of CFM fiber $d_f = 6 \times 10^{-6}$ m

$H \times 10^4$ (m)	H/d_f	$D_{react} \times 10^2$ (m)	D_{react}/d_f
4.0	66.7	1.98	3300
		1.44	2400
15.0	250	1.10	1800
		0.80	1300

plug-flow regime was realized under the experimental conditions. Hence, kinetics of the irreversible reaction of ozone decomposition could be described by the relationship

$$k\tau' = \ln \frac{C^{i}_{O_3}}{C^{f}_{O_3}}. \quad (4)$$

The initial experimental data on ozone decomposition over CFMs are presented as the time dependence of the final ozone concentration, i.e. ozone concentration in the reactor outlet, at different parameters (Fig. 1).

Such an appearance of kinetic curves is characteristic. It is repeated for all other series of experiments with both, low and high initial ozone concentration ($(2.1–6.2) \times 10^{-7}$ and $(0.5–3.1) \times 10^{-5}$ mol/l, respectively). The data shown in Fig. 1 have been obtained for ozone decomposition by SAF-4 at $C^{i}_{O_3} = 6.2 \times 10^{-7}$ mol/l when GAM linear velocity increased from 5.3 to 33.2 cm/s.

One can see that ozone concentration in the outlet of the adapter growing initially reaches a certain constant value. An analogous series of experiments has been carried out at the high ozone concentration ($C^{i}_{O_3} = 2.1 \times 10^{-5}$ mol/l). The data of the both series were transformed applying Eq. (4) (Fig. 2) and Eq. (1) (Table 3).

Linear dependences obtained for different $C^{i}_{O_3}$ regions (Fig. 2) prove the plug-flow regime of the reactor operation. As is obvious from Table 3, at low $C^{i}_{O_3}$, the reaction rate is limited by the external diffusion only at the initial period ($dW_0/dU > 0$) of the process, whereas *i*n a case of high $C^{i}_{O_3}$, the external diffusion can be neglected by either in the initial or at the steady-state period ($dW_{st}/dU = 0$) of the process.

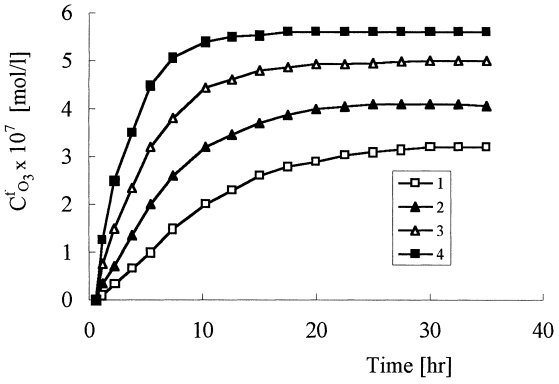

Fig. 1. The time dependence of the final ozone concentration ($C^{f}_{O_3}$) of ozone decomposition for SAF-4 sample at various GAM linear velocities, *U*: (1), 5.3; (2), 10.0; (3), 17.5; (4), 33.2 cm/s. Initial ozone concentration, $C^{i}_{O_3} = 6.2 \times 10^{-7}$ mol/l; humidity $\varphi = 60\%$; $T = 20°C$; volumetric flow rate $\omega = 1.7 \times 10^{-5}$ m^3/s.

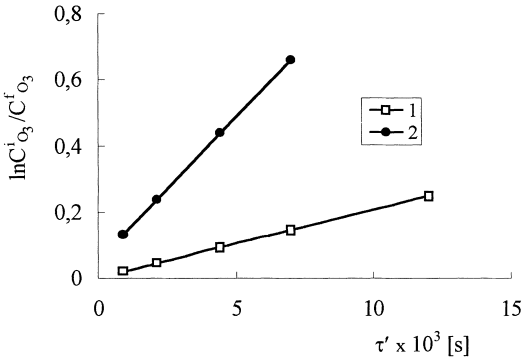

Fig. 2. Plot of $\ln C^{i}_{O_3}/C^{f}_{O_3}$ vs. the residence time (τ') of ozone decomposition by SAF-3 (1) and SAF-4 (2) samples in the steady-state regime at the initial ozone concentrations in GAM, $C^{i}_{O_3}$: (1), 2×10^{-5}; (2), 6.2×10^{-7} mol/l.

Table 3
Dependence of parameters of ozone decomposition by SAF-4 (run l) and SAF-3 (run 2) on GAM linear velocity under following conditions: $\varphi = 60\%$; $\omega = 1.7 \times 10^{-5}$ m^3/s; $T = 20°C$

U (cm/s)	$\tau' \times 10^3$ (s)	$W_0 \times 10^7$ (mol/g s)	$W_{st} \times 10^7$ (mol/g s)
Run 1: *SAF-4*; $C^{i} = 4.2 \times 10^{-7}$ (*mol/l*)			
5.3	7.5	0.9	0.33
10.0	4.0	1.7	0.44
17.5	2.3	3.0	0.46
33.2	1.2	5.6	0.43
Run 2: *SAF-3*; $C^{i} = 2.1 \times 10^{-5}$ (*mol/l*)			
5.3	7.5	25.0	8.7
10.0	4.0	40.0	8.5
17.5	2.3	40.0	8.3
33.2	1.2	40.0	8.4

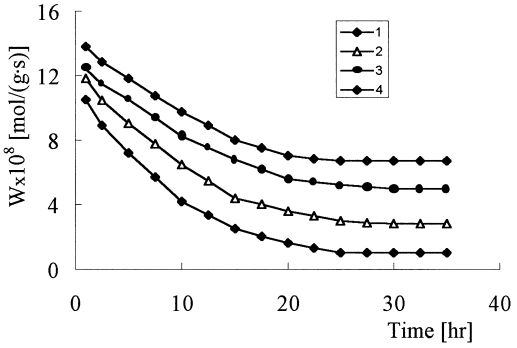

Fig. 3. The time dependence of ozone decomposition rate (W) for carbon fibrous materials with various V_{mi}/V_{me} ratios: (1), 6.8 (SAF-1); (2), 4.2 (SAF-2); (3), 3.3 (SAF-3); and (4), 3.0 (SAF-4). $C^{i}_{O_3} = 6.2 \times 10^{-7}$ mol/l; GAM linear velocity, $U = 5.3$ cm/s; humidity $\varphi = 60\%$; $T = 20^{\circ}$C; volumetric flow rate $\omega = 1.7 \times 10^{-5}$ m^3/s.

3.2. Influence of structural characteristics

As shown earlier [12], kinetics of ozone decomposition depends essentially on V_{mi}/V_{me} ratio. However, it has been deduced on the basis of experimental data obtained at constant U when the residence time of GAM was varied (CFMs differed in a layer thickness). In order to get a correct conception of the reaction parameters dependence on CFM structural characteristics, SAF 1–4 samples of the same thickness ($H = 4\times10^{-4}$ m) have been obtained. Since U was constant, all of them ensured the same effective residence time of GAM. Kinetic curves in W vs. Time plot (Fig. 3) are similar for SAF 1–4.

This indicates the similar character of ozone interaction with these CFMs, i.e. CFM activation leads to micro- and mesoporous structure development and does not change the character of surface-active centers. CFM power in ozone decomposition can be evaluated by the magnitude of its specific activity under the steady-state regime conditions, $\alpha_{st} = W_{st.}/(S_{mi} + S_{me})$ (Table 4).

As is obvious, *within the region of low ozone concentrations* (Table 4, run 1), W_{st} and the specific activity, α_{st}, increases as the V_{mi}/V_{me} ratio decreases as follows: SAF-1 < SAF-2 < SAF-3 < SAF-4. This can be evidence of the decrease of the internal-diffusion inhibition (which takes place in 'fine' pores) and the increase of the CFM surface portion taking part in ozone decomposition. The appropriateness obtained disproves the conception [23] that interaction of ozone with carbon materials occurs only on their external surface or on macropore walls. Since CFMs under study were characterized by practically constant volume of macropores ($V_{ma} = 0.35$ cm^3/g), the reaction acceleration in the steady-state regime depends on the development of micro- and mesoporosity.

Within the region of high $C^{i}_{O_3}$ (Table 4, run 2), in contrast to the previous data, CFM specific activity does not depend on the value of V_{mi}/V_{me} ratio. It can be evidence of the disappearance of the internal-diffusion inhibition of the gas-phase reaction and the dependence of the reaction rate on a character of surface active centers. Since the growth of basic groups concentration from 0.21 to 0.44 mmol/g for SAF 1–3 is accompanied by a certain increase in their W_{st}, the former can be considered as the cause of the latter. Under conditions eliminating the internal and external diffusion, the value of CFM specific activity depends only on the initial concentration of ozone in GAM and grows linearly along with the increase in $C^{i}_{O_3}$ (Fig. 4).

It is consistent with the dependence reported for ozone decomposition on Ag-pyrolusite catalyst at $C^{i}_{O_3}$ ranged from 4.0×10^{-6} to 4.5×10^{-5} mol/l [24]. To compare the activity demonstrated by various CFMs and catalysts in ozone decomposition reaction on the basis of the specific activity value, it is necessary to take into consideration the ozone concentration and a linear character of α_{st} vs. $C^{i}_{O_3}$ plot. For instance, applying the data previously reported [11], we have determined the specific activity of CFMs prepared of polyacrylonitril, $\alpha_{st} = 4.3\times10^{-12}$ mol/(m^2·s). One can deduce that CFMs applied in our investigation are much more active than those ones [11]. However, the activity of Ag-pyrolusite catalyst [24] was ten times the value observed for our CFMs.

3.3. $CuCl_2$–CFM as a catalyst of ozone decomposition

Carbon fibrous materials have been thoroughly -studied as supports of metal complex compounds in a case of Cu(II)–Hg(II) and Cu(II)–Pd(II) bifunctional catalysts of phosphine microconcentration oxidation [17]. A substantial increase in their catalytic activity has been shown to accompany the development of CFM porous structure. In general, ozone decomposition was studied over SiO_2-, Al_2O_3- and

Table 4
Dependence of ozone decomposition parameters on CFM (SAF) structural characteristics under following conditions: $U = 5.3$ cm/s; $\tau' = 7.5 \times 10^{-3}$ s; $\varphi_{GAM} = 60\%$; $T = 20^{\circ}C$

Sample	V_{mi}/V_{me}	$W_0 \times 10^7$ (mol/g s)	$W_{st} \times 10^7$ (mol/g s)	$\alpha_{st} \times 10^{10}$ mol/(m^2.s)
Run 1: $C^i = 6.2 \times 10^{-7}$ (*mol/l*)				
SAF-1	6.8	1.1	0.1	0.1
SAF-2	4.2	1.2	0.3	0.3
SAF-3	3.5	1.2	0.6	0.4
SAF-4	3.0	1.4	0.7	0.5
Run 2: $C^i = 3.2 \times 10^{-5}$ (*mol/l*)				
SAF-1	6.8	42.6	5.4	6.7
SAF-2	4.2	46.0	7.1	7.2
SAF-3	3.5	60.0	9.3	7.3

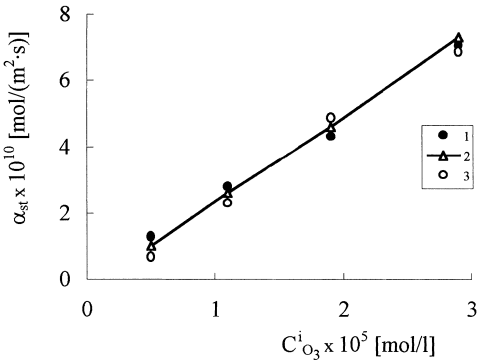

Fig. 4. Dependence of CFM specific catalytic activity (α_{st}) on $C^i_{O_3}$ in GAM regarding ozone decomposition in the steady-state regime for various V_{mi}/V_{me} ratios: (1), 6.8 (SAF-1); (2), 4.2 (SAF-2); (3), 3.3 (SAF-3); GAM linear velocity, $U = 5.3$ cm/s; humidity $\varphi = 60\%$; $T = 20^{\circ}C$.

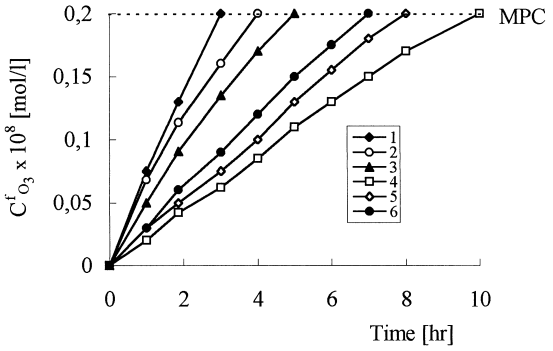

Fig. 5. The time dependence of $C^f_{O_3}$ of ozone decomposition by $CuCl_2$–SAF-1 systems with various catalyst concentrations, $[CuCl_2] \times 10^{-4}$, mol/g: (1), 0; (2), 0.5; (3), 1.0; (4), 2.5; (5), 5.0; (6), 10.0. $C^i_{O_3} = 3.2 \times 10^{-8}$ mo/l; GAM linear velocity U=5.3 cm/s; humidity $\varphi = 60\%$; $T = 20^{\circ}C$.

AC-supported metal complex catalysts [4–7]. The data on the dependence of kinetics of ozone decomposition on C_{CuCl_2} and CFM porous structure are presented in this work.

At $C^i_{O_3} \geq 2.1 \times 10^{-5}$ mol/l, a catalytic effect of copper(II) chloride was very weak for both, the low-porous (SAF-1) and high-porous (SAF-4) supports. A degree of ozone decomposition was not more than 30–35% in the steady state regime. A considerable copper(II) influence was founded at $C^i_{O_3} \geq 3.2 \times 10^{-8}$ mol/l. To characterize the catalyst activity within this concentration region, τ_{MPC} parameter (the time necessary for reaching of ozone maximum permissible concentration (MPC_{O_3})) was used. In accordance with Ukrainian standard, $MPC_{O_3} = 2 \times 10^{-9}$ mol/l.

Copper(II) chloride content in $CuCl_2$–SAF-1 system was varied from 0 to 1.0×10^{-3} mol/g (Fig. 5).

The curves were of the same appearance at various C_{CuCl_2} values: the final ozone concentration increased up to MPC_{O_3} and, then, the test was stopped. Only a part of experimental results is shown in Fig. 5. More detailed data of τ_{MPC}, V_{mi} and β dependence on C_{CuCl_2} are summarized in Table 5.

One can see that the increase of copper(II) chloride content is accompanied by the decrease of the volume of micropores. It is evidence of the distribution of the catalytic addition not only on the external but also on the internal CFM surface [25]. The saturation degree of CFM surface grows; τ_{MPC} reaches its maximum value (10 h) at $C_{CuCl_2} = 2.5 \times 10^{-4}$ mol/g. Judging from V_{mi} and β values, the decrease of τ_{MPC} $C_{CuCl_2} > 2.5 \times 10^{-4}$ mol/g is due to $CuCl_2$ blockage of

Table 5
Specific volume of micropores (V_{mi}), saturation degree of CFM surface with $CuCl_2$ (β) and time of protective action (τ_{MPC}-) of $CuCl_2$–SAF-1 catalyst dependences on C_{CuCl_2} under following conditions: $U = 5.3$ cm/s;$C^i = 3.2 \times 10^{-8}$ mol/l; $T = 20°C$; $\varphi_{GAM} = 60\%$; $a_{m(Cu)} = 2.1 \times 10^{-4}$ mol/g

$C_{CuCl_2} \times 10^4$ (mol/g)	V_{mi} (cm^3/g)	β	τ_{MPC} (h)
0	0.240	0	4
0.5	0.228	0.24	5
1.0	0.219	0.48	6
2.0	0.205	0.96	8
2.5	0.193	1.20	10
5.0	0.180	2.40	8
10.0	0.170	4.80	7

considerable portion of SAF-1 surface and to the formation of polylayers consisting of $CuCl_2$ molecules. This is characteristic for other CFM samples [26], too. As a result, lowering of the $CuCl_2$–SAF-1 catalyst activity was observed. A similar dependence has been obtained for $CuCl_2$–$HgCl_2$–CFM catalyst tested in oxidation of phosphine microconcentrations by oxygen [17].

The appearance of curves of ozone decomposition in $C^f_{O_3}$ vs. Time plot for $CuCl_2$–SAF-4 catalyst (SAF-4 is notable with its developed micro- and mesoporous structure) depends on copper(II) chloride content (Fig. 6).

As an example, at $C_{CuCl_2} = 5.0 \times 10^{-5}$ mol/g, at first, τ_{MPC} decreases insignificantly as compared with the initial SAF-4 sample, whereas it is twice the latter already at $C_{CuCl_2} = 1.0 \times 10^{-4}$ mol/g. The steady-state regime of ozone decomposition with $C^f_{O_3} < MPC_{O_3}$ is observed for C_{CuCl_2} ranged from 2.5×10^{-4} to 2.5×10^{-3} mol/g.

For $CuCl_2$–SAF-4 catalyst, changing of V_{mi} and β parameters was similar to that for the $CuCl_2$–SAF-1 catalyst. However, the distinguishing feature of $CuCl_2$–SAF-4 catalyst was the formation of copper(II) hydroxo complex, Cu(OH)Cl, on the CFM surface as a result of a high content of basic groups proved by high pH value of water extract (see Table 1). For SAF-1, hydrolysis of copper(II) chloride was not observed. As a rule, an alterations in the composition of metal complex coordination sphere results in changing its catalytic activity in redox reactions of O_3, PH_3, CO and other toxic gaseous molecules [27].

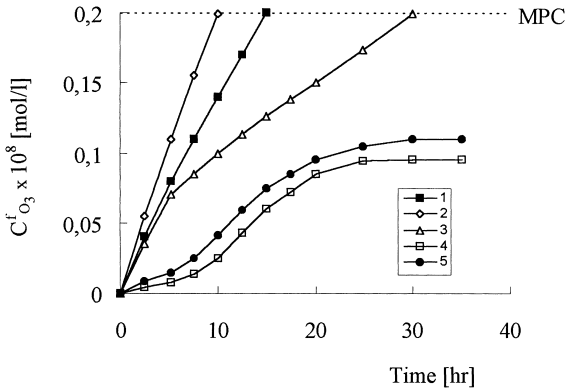

Fig. 6. The time dependence of $C^f_{O_3}$ of ozone decomposition by $CuCl_2$–SAF-4 system with various catalyst concentrations, $[CuCl_2] \times 10^4$ mol/g: (1), 0; (2), 0.5; (3), 1.0; (4), 2.5; (5), 25.0. $C^i_{O_3} = 3.2 \times 10^{-8}$ mol/l; GAM linear velocity $U = 5.3$ cm/s; humidity $\varphi = 60\%$; $T = 20°C$.

Table 6
Dependence of τ_{MPC} on φ_{GAM} in ozone decomposition by CFMs and $CuCl_2$–CFM catalysts under following conditions: U=5.3 cm/s; $C^i = 3.2 \times 10^{-8}$ mol/l; $T = 20°C$

φ_{GAM} (%)	τ_{MPC} (h)	System
30	6.0	SAF-1
60	4.0	
90	2.0	
30	12.0	$CuCl_2$–SAF-1
60	10.0	$C_{CuCl_2} = 2.5 \times 10^{-4}$ mol/g
90	8.0	
10	7.0	SAF-4
20	9.0	
60	12.0	
10	21.0	$CuCl_2$–SAF-4
20	25.0	$C_{CuCl_2} = 5 \times 10\_^5$ mol/g
60	32.0	

3.4. Influence of GAM humidity

The data concerning τ_{MPC} dependence on φ_{GAM} for both, SAF-1 and SAF-4 samples, and $CuCl_2$–CFM catalysts are summarized in Table 6.

One can see that φ_{GAM} growth is accompanied by τ_{MPC} decrease for SAF-1 and $CuCl_2$–SAF-1 samples and the τ_{MPC} increase for SAF-4 and $CuCl_2$–SAF-4 samples. Such a difference can be explained by the different character of the supports and the ratio of their functional groups as well as by supported metal

complex composition. The activity growth observed for the particular catalysts with the increase of GAM humidity is caused, in our opinion, by the presence of only basic surface groups and alkaline medium in the layer of water adsorbed in a case of SAF-4 (see Table 1) as well as the presence of hydroxo groups in the metal complex composition (i.e. Cu(OH)Cl formation).

3.5. On mechanism of ozone decomposition

The appearance of kinetic curves (see Figs. 1 and 3) characteristic for ozone decomposition is evidence of intricate processes which take place both, in the unsteady-state regime ($C^{f}_{O_3}$ grows and the reaction rate decreases) and in the steady-state regime ($C^{f}_{O_3}$ and W are constant). A similar kinetics was observed for ozone decomposition by active charcoals [23] and by Hopcalite-type, Pt/Al_2O_3- and Pd/Al_2O_3-catalysts [28]. The attainment of the steady-state regime is one of signs of ozone catalytic decomposition according to the reaction:

$$2\ O_3 \rightarrow 3\ O_2.$$

In the case of CFMs, one cannot exclude: (1) carbon oxidation to CO and CO_2; and (2) carbon oxidation accompanied with the formation of surface oxides with ion-exchange properties. However, even if ozone concentration is high ($C_{O_3} = 0.5$ vol%), only 20% of ozone is consumed in CFM surface oxidation accompanied with the formation of functional groups of various origins and the rest (ca. 80%) is decomposed over CFMs catalytically [11].To determine possible ways of ozone interaction with CFMs we (1) in every case, calculated the amount of ozone (V_{O_3} cm^3/g) reacted until the steady-state regime attainment; (2) made check measurements of CO and CO_2 concentration in GAM in the reactor outlet as well as CO_2 concentration in GAM in the reactor inlet; and (3) made check measurements of acidic and basic groups content of CFMs before, and after, the experiment realization. The examples of these data for SAF 1-3 samples are presented in Table 7.

These data permit to deduce that V_{O_3} exceeds by far the total volume of CFM pores (V_Σ, cm^3/g). Providing the volume of pores completely filled up with ozone, $n = V_{O_3}/V_\Sigma$ increases for SAF 1–3 samples. The gas chromatograph applied for measuring of carbon oxides concentration in GAM did not registered CO appearance and difference in CO_2 concentration (ΔC_{CO_2}). The content of acidic and basic surface groups did not differ from the initial one within the error of titration method. The authors do not exclude the appearance of other surface groups, but, accordingly to data reported [11], their portion is insignificant in comparison with above-mentioned ones. All things considered, one can come to the conclusion that not only adsorption processes and the adsorption equilibrium appointment are at the bottom of the characteristic appearance of the kinetic curves (the steady-state regime appointment). The latter is due to ozone catalytic decomposition over CFM active centers.

Judging by data available in the literature, the increase of the final ozone concentration in the region of unsteady-state kinetics, when the process, as a whole, is catalytic, can depend on many reasons: (1) CFM graphitization at high ozone concentration ($\geq$5 vol%) and the decrease of the accessible surface area [11]; (2) as a result of the oxidation process, formation of water molecules blocking active centers of CFM surface [29]; and (3) formation of atomic oxygen with its subsequent strong bonding to CFM surface [30]. The first and second reasons can be neglected under our experimental conditions (low ozone concentration, different dependencies of ozone decomposition process on water due to a character of CFM functional groups). Since the attempt to regenerate under mild conditions ($T = 110$°C) CFM initial activity lost in the process failed, the blockage of the surface with atomic oxygen can not be excluded.

In fact, a question of a nature of CFM active centers is not discussed in the available literature. Carbon atoms and double bonds are considered as taking part in ozone decomposition by active carbons [23]. In our opinion, since all SAFs contain basic surface groups (in a case of SAF 3–6, basic surface groups only) and CFM hydrophilicity is high, the participation of hydrated OH group in ozone decomposition is most probable. It is conformed with mechanism of ozone decomposition in water and weak-alkaline aqueous solutions [31–34] and with the conclusion [35,36] that hydroxo groups of some oxide catalysts (Fe_2O_3 and TiO_2) participate in ozone decomposition. Furthermore, the data on ozone adsorption on some

Table 7
Data for determination of a possible reaction pathway of oznone decomposition under following conditions: $\omega = 1.7 \times 10^{-5}$ m^3/s; $U = 5.3$ cm/s; $C^i = 3.1 \times 10^{-5}$ mol/l; $T = 20^\circ$C; $\varphi_{GAM} = 60\%$

Sample	V_Σ (cm^3/g)	V_{O_3} (cm^3/g)	n	A_a (mmol/g)	A_b (mmol/g)	C_{CO}	ΔC_{CO_2}
SAF-1	0.27	18.6	69.0	0.46 ± 0.03	0.21 ± 0.02	absent	0
SAF-2	0.37	102.7	277.0	0.15 ± 0.01	0.40 ± 0.03	absent	0
SAF-3	0.43	140.6	327.0	absent	0.44 ± 0.03	absent	0

oxides (SiO_2 and TiO_2) [2] prove ozone interaction with surface hydroxo group as well as with Lewis acceptor centers.

The mechanism of ozone decomposition over silica-supported complex compounds of Cu(II) was earlier discussed by us in detail [37]. The reaction has been shown to occur including the stage of intraspheric redox transformation of metal complex-ozone molecule intermediate. The difference in activity of CFM-supported chloro and hydroxochloro Cu(II) complexes confirms this mechanism of ozone decomposition.

4. Conclusions

For the first time, kinetics of low-temperature ozone decomposition by woven carbon fibrous materials obtained from raw cellulose under conditions permitting the purposeful control of a porous structure, a character and a ratio of surface groups was investigated in the wide range of ozone concentration (from 3.1×10^{-8} to 3.1×10^{-5} mol/l). It has been shown that CFMs with a developed porous structure and a high content of basic functional groups are effective catalysts of ozone decomposition and optimal supports of metal complex catalysts, e.g. copper(II) chloride. The catalysts under study differ advantageously from the ones generally used. The difference is in the increase of the activity of the former with a growth of GAM humidity and the content of CFM-adsorbed water. When ozone decomposition over CFMs occurs in the kinetic region, their activity can be characterized by such a quantitative criterion as the specific catalytic activity. This criterion does not depend on CFM porous structure and increases linearly with ozone concentration growth other things being equal.

5. Symbols and abbreviations

A_a	content of acidic groups (mmol/g)
A_b	content of basic groups (mmol/g)
a_{st}	CFM static activity (mg/g)
$a_{m(Cu)}$	specific Cu(II) monolayer capacity on CFM (mol/g)
AC	active charcoal
BAM	benzene-air mixture
C^f	final ozone concentration in GAM, (mol/l), (mol/m^3)
C^i	initial ozone concentration in GAM (mol/l), (mol/m^3)
CFM	carbon fibrous material
d_f	diameter of CFM fiber (m)
d_g	grain diameter (m)
D_{react}	inner reactor diameter (m)
GAM	gas-air mixture
H	height of the catalyst layer (m)
m	CFM sample weight (g)
m_{H_2O}	amount of water adsorbed (g/g)
MPC_{O_3}	maximum permissible concentration of ozone (mol/l), (mg/m^3)
$n = V_{O_3}/V_\Sigma$	turnover number
S_a	geometric area of CFM cross section fitting the orifice in the adapter (cm^2)
S_{me}	specific surface of CFM mesopores (m^2/g)
S_{mi}	specific surface of CFM micropores (m^2/g)
SAF	CFM type (sorption-active fabric)
T	temperature ($^\circ$C)

U	GAM linear velocity (cm/s)
V	total volume of the catalyst layer (cm^3)
V_{ma}	specific volume of macropores (cm^3/g)
V_{me}	specific volume of mesopores (cm^3/g)
V_{mi}	specific volume of micropores (cm^3/g)
V_{O_3}	specific amount of ozone reacted until the steady-state regime attainment (cm^3/g)
V_Σ	total specific volume of CFM pores (cm^3/g)
W	rate of ozone decomposition (mol/g s)
W_0	initial rate of ozone decomposition (mol/g s)
W_{st}	rate of ozone decomposition in the steady state regime, mol/(g s)
$\alpha_{st} = W_{st}/(S_{mi} + S_{me})$	specific activity of CFM under the steady-state regime conditions (mol/(m^2 s)
β	saturation degree of CFM surface with $CuCl_2$
ΔC_{CO_2}	difference in CO_2 concentration in the inlet and in the outlet of the reactor (vol%)
φ	GAM humidity (%)
τ_{MPC}	time of protective action (the time necessary for reaching of ozone maximum permissible concentration (MPC_{O_3})) (h)
τ'	effective residence time of GAM (s)
σ	area by one Cu(II) ion (cm^2)
ω	GAM volumetric flow rate (m^3/s)

Acknowledgements

The authors acknowledge the partial support of this work by ISSEP (Grant Nos. PSU 053010 and QSU 083159).

References

[1] A.N. Nikonorov. Sources of Ozone in Exhausted Gases and Methods of its Removal, TsINTIKhimneftemash, Moscow, 1985, p. 25.
[2] B. Dhandapani, S.T. Oyama, Appl. Cat. B: Environm. 11 (1997) 129.
[3] T.L. Rakitskaya, A.A. Ennan, V.Ya. Paina. Catalysts of Low-Temperature Carbon Monoxide Oxidation, TsINTIKhimneftemash, Moscow, 1991, p. 36.
[4] S.V. Osintseva, L.E. Gorlenko, G.I. Emelianova, L.D. Kvatcheva, Yu.N. Novikov, M.E. Vol'pin, Zhurn. Fiz. Khim. 63 (1989) 3228.
[5] V.F. Zackay, D.R. Rowe, Great Britain Patent, 2142324 (1985).
[6] Takeda Yakuchin Koge K.K., Japan Patent 53-45712 (1978).
[7] T.L. Rakitskaya, I.V. Granatyuk, G.G.A. Balovoin, Yu.V. Geletii, A.A. Golub, L.A. Raskola, in 'Silica-98: An International Conference on Silica Science and Technology, Mulhous, France, 1–4 September, 1998, Mulhous, 1998, 653 p.
[8] Ch. Heisig, W. Zhang, S.T. Oyama, Appl. Cat. B: Environm. 14 (1997) 117.
[9] L.F. Atyaksheva, G.I. Emel'yanova, Vestn. Mosk. Univ. Ser.2. Khimiya 24 (1983) 462.
[10] L.F. Atyaksheva, G.I. Emel'yanova, T.S. Lazareva, Mekh. Kompozits. Mater. 1 (1988) 166.
[11] G.I. Atyaksheva, L.F. Emel'yanova, Zhurn. Fiz. Khim 63 (1989) 2606.
[12] T.L. Rakitskaya, A.Yu. Bandurko, V.V. Litvinskaya, Zhurn. Prikl. Khim. 66 (1993) 2141.
[13] T.L. Rakitskaya, A.Yu. Bandurko, A.A. Ennan, Kinet. Katal. 35 (1994) 763.
[14] T.L. Rakitskaya, A.Yu. Bandurko, O.V. Boginskaya, Zhurn. Prikl. Khim. 69 (1996) 167.
[15] T.L. Rakitskaya, A.A. Ennan, A.Yu. Bandurko, V.V. Litvinskaya, Bezopasnost' truda v promyshlennosti 6 (1993) 19.
[16] T.L. Rakitskaya, A.A. Ennan, A.Yu. Bandurko, Avtomat. svarka 7 (1995) 62.
[17] T.L. Rakitskaya, A.A. Ennan, T.D. Red'ko, N.N. Abramova, V.V. Litvinskaya, Zhurn. Prikl. Khim. 70 (1997) 466.
[18] M.M. Dubinin, Dokl. Akad. Nauk SSSR 275 (1984) 1442.
[19] M.M. Dubinin, L.I. Katayeva, N.S. Polyakova, Izv. Akad. Nauk SSSR. Ser. Khim. 7 (1987) 1453.
[20] H.P. Boehm, Adv. Catal. Relat. Subj. 16 (1966) 174.
[21] G.K. Boreskov, Catalysis, Nauka SO Akad. Nauk SSSR, Novosibirsk, 1971, 268 p.
[22] Yu.Sh. Matros, Unsteady-State Processes in Catalytic Reactors, Nauka SO Akad. Nauk SSSR, Novosibirsk, 1982, 234 p.
[23] V.R. Dietz, J.L. Bitner, Carbon 11 (1973) 393.
[24] V.Ya. Vol'fson, A.F. Sudak, V.M. Vlasenko, Kinet. Katal. 23 (1982) 84.
[25] T.L. Rakitskaya, V.V. Litvinskaya, T.D. Red'ko, Zhurn. Prikl. Khim. 60 (1987) 1415.
[26] T.L. Rakitskaya, T.D. Red'ko, V.V. Litvinskaya, Zhurn. Prikl. Khim. 65 (1992) 1977.

[27] D.V. Sokol'skiy, Ya.A. Dorfman, T.L. Rakitskaya, Proton-aproton catalysis in solutions, Nauka, Alma-Ata, 1975, 245 p.
[28] M.P. Popovich, N.N. Smirnova, Yu.V. Filippov, Vestn. Mosk. Univ. Ser.2. Khimiya 26 (1985) 167.
[29] V.G. Oleynikov, B.B. Donster, T.N. Burushkina, Khim. Tekhnol. 1 (1989) 12.
[30] G.I. Golodets, Heterogeneous Catalytic Reactions with Participation of Molecular Oxygen, Naukova dumka, Kiev, 1977, 359 p.
[31] H. Tamiyasu, H. Furutomi, G. Gordon, Inorg. Chem. 24 (1985) 2962.
[32] J.L. Sotelo, F.J. Beltran, F.J. Benitez, J. Beltran-Haredia, Ind. Eng. Chem. Res. 27 (1988) 548.
[33] A.D. Nadezhdin, Ind. Eng. Chem. Res. 26 (1987) 39.
[34] A. Virds, A. Viola, Ann. Chim (Soc. Chim. Ital.) 85 (1995) 633.
[35] N.D. Dobroskina, Yu.I. Shulyatskiy, I.N. Kamenchuk, Trudy Mosk. Khim.-Tekhn. Inst. 119 (1981) 119.
[36] B. Ohtani, Sh.-W. Zhang, S. Nichimoto, Y. Kagiva, J. Chem. Soc. Faraday Trans. 88 (1992) 1049.
[37] T.L. Rakitskaya, L.A. Raskola, V.Ya. Paina,, A.Yu. Bandurko, Izv. VUZov. Khimiya i khim. technologiya 42 (1999) 39.